Hydrodynamics of a Water Rocket*

Joseph M. Prusa†

Abstract. Applications of mass, momentum, and energy balances are central to the teaching of fluid dynamics. In this study, a model to determine the trajectory of a water rocket is given that is far simpler than the system of coupled partial differential equations that typically results in modern hydrodynamic problems of interest. This makes the problem an excellent choice for a student project—it can reasonably be completed with a day or two of effort. In addition to the fundamental mathematics, this problem offers opportunities in scale analysis, numerical methods for IVPs, balance principles in accelerated frames of reference, and the collection and assessment of flight test data.

Key words. hydrodynamics, predictor-corrector, nonlinear integral equation, rocket thrust, adiabatic expansion, noninertial frame

AMS subject classifications. 65-01, 65L05, 65L12, 65L80, 76-01, 80-01

PII. S0036144598348223

1. Introduction. Many of us have enjoyed playing with a toy water rocket (Figure 1). The basic principle of operation is to expel a jet of water from the rocket nozzle using compressed air. After a volume of water has been poured into the interior chamber of the rocket, it is mounted on a hand pump and the chamber contents are compressed to several times atmospheric pressure. In a classic example of engineering elegance, when the rocket is pointed upwards for launch, gravity naturally stratifies the contents of the rocket so that the air cannot escape until it pushes all of the water out of the interior chamber. In this manner the stored energy of the air is efficiently transformed into kinetic energy of the exiting water jet. This jet provides sufficient thrust to propel the rocket to astonishing heights. A few trial launches quickly confirm that maximum heights are achieved with an intermediate volume of water. Due to its low density, the thrust provided by air alone is negligible, and in a launch without water, the rocket is barely able to lift off of the air pump seal. The other extreme consists of completely filling the chamber with water. In this case, the chamber cannot be pressurized since water is incompressible; consequently there is no stored energy to turn into kinetic energy.

Detailed predictions of the rocket trajectory are possible using a model based upon hydrodynamic principles. But what is remarkable is that because the design so efficiently transforms stored energy into thrust, the model can be simple enough to use as a project or take-home quiz in fluid dynamics at the advanced undergraduate or beginning graduate level. When coupled with actual flight test data, where the
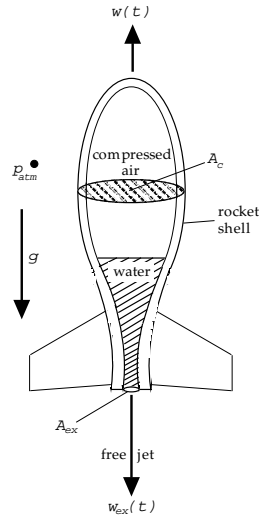
Fig. 1 *Water rocket schematic.*

class goes outside and measures the height and time of the trajectories, enthusiasm becomes palpable. This modeling exercise provides a great opportunity for students to bring together their skills in physical reasoning, analysis, and numerical methods. And it is fun!

2. Model. Application of Newton's second law to the rocket as viewed from inertial space $\mathbf{I_o(x_o)}$ (see Figure 2) yields $d\mathbf{P}/dt = m\mathbf{a_o}$, where $d\mathbf{P}/dt \equiv \mathbf{F}$ is the net force acting on the rocket ($\mathbf{P}$ is momentum), m is its mass, and $\mathbf{a_o}$ is its acceleration. It is convenient to compute the thrust in a frame of reference moving with the rocket, $\mathbf{I(x)}$ such that $\mathbf{R}(t) = \mathbf{I(0)} - \mathbf{I_o(0)}$ is the position vector of $\mathbf{I(0)}$ with respect to inertial space. In the noninertial space, Newton's second law generalizes to $d\mathbf{P}/dt = \mathrm{m}(\mathbf{a} + \ddot{\mathbf{R}})$, where $\ddot{\mathbf{R}} = d^2\mathbf{R}/dt^2$ is the rectilinear acceleration of $\mathbf{I(0)}$ in $\mathbf{I_o(x_o)}$ and $\mathbf{a}$ is the rocket's acceleration relative to $\mathbf{I(x)}$. Noting that $\mathbf{a} = \mathbf{0}$ (by definition of $\mathbf{I(x)}$), this Lagrangian description of the momentum balance is reformulated into an integral Eulerian description[1] using the Reynolds transport theorem [1]:

$$(2.1) \qquad \mathbf{F_s} - \mathbf{W} - m\ddot{\mathbf{R}} = \frac{\partial}{\partial t}\int_V \rho\mathbf{u}dV + \oint_A \rho\mathbf{u}(\mathbf{u}\cdot d\mathbf{A}),$$

where V is the control volume consisting of the interior of the rocket and its rigid shell, A is the surface of V, and $d\mathbf{A} \equiv \mathbf{n}dA$ is the vector surface area element of A with the direction of the outward pointed unit normal $\mathbf{n}$. Here $\mathbf{u}$ is velocity relative to

---

[1]Equation (2.1) represents an exact momentum balance that is equivalent to the more common partial differential equation representation commonly known as the Navier–Stokes equations. The weight and rectilinear acceleration terms on the left-hand side of (2.1) can be replaced with volume integrals (of $-\rho\mathbf{g}dV$ and $-\rho\ddot{\mathbf{R}}dV$, respectively), and the divergence theorem [2] can be used to convert the momentum flux term into a volume integral (of $\nabla\cdot(\rho\mathbf{uu})dV$). Assuming that V is independent of time (but otherwise unspecified) allows $\partial/\partial t$ to be moved inside the first integral on the right-hand side of (2.1). The surface force can be written as a volume integral of the divergence of the total stress tensor ($(\nabla \cdot \mathbf{S})dV$). By combining all integrands and using the fundamental lemma of the variational calculus [3], the Navier–Stokes equations in noninertial coordinates [4] are generated.
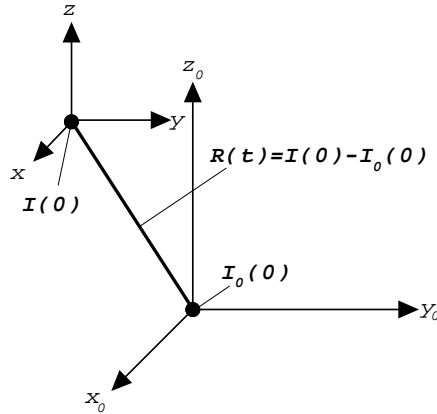
Fig. 2 *Inertial and noninertial frames of reference.*

$I(x)$, $\mathbf{W} \equiv m\mathbf{g}$ is the weight of the rocket, and $\mathbf{F_s}$ represents surface forces. The first integral on the right-hand side of (2.1) represents the rate of increase of momentum of the control volume with respect to the noninertial space, and in this case is zero (by definition, the velocity of the control volume is $\mathbf{u} \equiv \mathbf{0}$). The second integral represents the net momentum efflux through the control surface; it is the thrust term.

Assuming that (i) the launch is directed straight up (which can be reasonably approximated in practice given sufficient care), (ii) the jet outflow has uniform properties across the exit area A_{ex} of the nozzle, and (iii) the only surface force acting on the rocket is drag, (2.1) reduces to

$$(2.2) \qquad \ddot{z} = (\rho_w w_{ex}{}^2 A_{ex})/m - \rho_{atm} A_c C_d w^2/2 - g,$$

where z is the rocket altitude (in $\mathbf{I_o}(\mathbf{x_o})$), ρ_w is the density of water, and w_{ex} is the jet exit velocity relative to the control surface (e.g., downward velocity in $\mathbf{I}(\mathbf{x})$), whereas w is the rocket velocity (e.g., vertical velocity in $\mathbf{I_o}(\mathbf{x_o})$). The drag coefficient is denoted by C_d and the density of the surrounding atmosphere by ρ_{atm}, and A_c is the cross-sectional area of the rocket in the plane perpendicular to the vertical. First and second integrals of (2.2) produce the vertical velocity and altitude of the rocket in $\mathbf{I_o}(\mathbf{x_o})$, respectively:

$$(2.3\mathrm{a,b}) \qquad w = \int_0^t \ddot{z}\,d\tau \quad \text{and} \quad z = z_o + \int_0^t w\,d\tau.$$

The z_o term compensates for launches from other than ground level.

In order to integrate (2.2), the jet exit velocity w_{ex} and rocket mass must first be determined. For any control volume V an integral mass balance can be written in the form

$$(2.4) \qquad 0 = \frac{\partial}{\partial t} \int_V \rho\,dV + \oint_A \rho(\mathbf{u} \cdot d\mathbf{A}).$$

Here the first integral on the right-hand side represents the rate of increase of mass in V, while the second integral gives the net mass efflux across A. This result is also exact and can be shown to be fully equivalent to the continuity equation using

the divergence theorem and fundamental lemma of the variational calculus. For the rocket problem, with the control volume consisting of the interior of the rocket and its rigid shell, (2.4) reduces to

$$(2.5) \qquad V_a(t) = V_a(0) + A_{ex} \int_0^t w_{ex} d\tau,$$

where $V_a(t) = V_{tot} - V_w(t)$ is the volume of compressed air in the chamber, V_{tot} is the total chamber volume, and $V_w(t)$ is the volume of water remaining in the chamber. The rocket mass is given by

$$(2.6) \qquad m(t) = m_s + m_a + \rho_w[V_{tot} - V_a(t)].$$

Here m_s is the mass of the rocket shell and m_a is the mass of compressed air trapped in the rocket chamber. This latter mass is constant during the thrust period and equal to $[p_a(0)V_a(0)]/[R_aT_a(0)]$, where $p_a(0)$, $T_a(0)$, and R_a are the initial pressure and temperature of the compressed air and air gas constant, respectively.

The jet exhaust velocity is determined by the transformation of stored energy of the pressurized air into kinetic energy of the water jet. For inviscid, incompressible, and steady flow along a streamline, an exact integral of the energy equation is Bernoulli's equation [4]. The incompressibility condition is met by taking a streamline from the compressed air/water interface in the rocket chamber, at pressure $p_a(t)$, down through the volume of water to the exit plane of the nozzle, at atmospheric pressure p_{atm}. The inviscid condition is met by an efficient[2] nozzle design. The final condition of steady flow is not rigorously met, but comparison of the time scales for unsteadiness ($\tau_{un} \sim 0.1\ s$) versus advection of the water ($\tau_{adv} \sim l/w_{ex} \sim 0.001\ s$) shows that the process is quasi-steady. Here $l \sim 0.01\ m$ is a characteristic length for the rocket chamber, and $w_{ex} \sim 10\ ms^{-1}$ from the model results. The unsteady time scale corresponds to the period of thrust and is determined by direct observation (or model results). Hence all the conditions for Bernoulli's equation are reasonably met. Assuming that the kinetic energy at the compressed air/water interface is negligible, the following expression for jet velocity results:

$$(2.7) \qquad w_{ex} = \sqrt{2[p_a(t) - p_{atm}]/\rho_w}.$$

Closure of the problem is achieved by determining the compressed air pressure. This requires knowledge about the nature of the expansion process. The expansion is very fast with respect to time scales for heat transfer ($\tau_{un} \ll \tau_{ht} \sim l^2/\alpha \sim 10\ s$, where $\alpha \sim 10^{-5}\ m^2 s^{-1}$ is the thermal diffusivity of the air), so an adiabatic approximation is a good one to choose. Adiabatic expansion of an ideal gas with constant specific heats gives [4]

$$(2.8) \qquad p_a(t) = p_a(0)[V_a(0)/V_a(t)]^\gamma,$$

where $\gamma \equiv c_p/c_v$ is the ratio of specific heats. Equations (2.5), (2.7), and (2.8) may be combined to give the nonlinear integral equation [5]

$$(2.9) \qquad V_a(t) = V_a(0) + A_{ex} \int_0^t \sqrt{2(p_a(0)[V_a(0)/V_a(t)]^\gamma - p_{atm})/\rho_w}\ d\tau.$$

---

[2]Theoretically, a 100% efficient nozzle design is one for which there is no entropy production. In the present example this means the expanding flow satisfies Bernoulli's equation exactly. From a practical viewpoint, efficient nozzle designs require smooth duct flow surfaces with no rapid changes in cross-sectional area. See the discussion of (2.7′) in section 5.

3. Solution. Equations (2.2), (2.3), and (2.5)–(2.8) with specified initial conditions $V_w(0)$ and $p_a(0)$ and parameters V_{tot}, m_s, A_{ex}, γ, R_a, p_{atm}, ρ_w, $T_a(0)$, g, and z_o complete the model that describes the rocket trajectory. Since the problem is strongly nonlinear, a numerical method is used to solve the model equations. The initial conditions take on the form

(3.1a–h)

$$t^0 = 0, \quad p_a{}^0 = p_a(0), \quad V_a{}^0 = V_{tot} - V_w(0), \quad w_{ex}{}^0 = \sqrt{2(p_a{}^0 - p_{atm})/\rho_w},$$

$$m^0 = m_s + [p_a{}^0 V_a{}^0]/[R_a T_a(0)] + \rho_w V_w(0), \quad \ddot{z}^0 = [\rho_w (w_{ex}{}^0)^2 A_{ex}]/m^0 - g,$$

$$w^0 = 0, \quad \text{and} \quad z^0 = z_o.$$

Given all relevant variables at time level n, where $t^n = (n-1)\Delta t$ is the corresponding time and Δt the timestep, the following predictor-corrector scheme is used to compute the solution during the thrust period at time level $n+1$:

(3.2a–e)

$$\widetilde{V}_a = V_a{}^n + A_{ex} w_{ex}{}^n \Delta t, \quad \widetilde{p}_a = p_a{}^0 [V_a{}^0/\widetilde{V}_a]^\gamma, \quad \widetilde{w}_{ave} = w^n + \ddot{z}^n \Delta t/2,$$

$$\widetilde{p}_{ave} = (p_a{}^n + \widetilde{p}_a)/2, \quad \text{and} \quad \widetilde{w}_{ex} = \sqrt{2(\widetilde{p}_{ave} - p_{atm})/\rho_w},$$

(3.2f–l)

$$V_a{}^{n+1} = V_a{}^n + A_{ex} \widetilde{w}_{ex} \Delta t, \quad p_a{}^{n+1} = p_a{}^0 [V_a{}^0/V_a{}^{n+1}]^\gamma,$$

$$w_{ex}{}^{n+1} = \sqrt{2(p_a{}^{n+1} - p_{atm})/\rho_w}, \quad m^{n+1} = m_s + m_a + \rho_w(V_{tot} - V_a{}^{n+1}),$$

$$\ddot{z}^{n+1} = [\rho_w (w_{ex}{}^{n+1})^2 A_{ex}]/m^{n+1} - \rho_{atm} A_c C_d{}^{n+1} (\widetilde{w}_{ave})^2 - g,$$

$$w^{n+1} = w^n + (\ddot{z}^n + \ddot{z}^{n+1})\Delta t/2, \quad \text{and} \quad z^{n+1} = z^n + (w^n + w^{n+1})\Delta t/2.$$

Equations (3.2a–e) consist of first-order predictions for the compressed air volume and pressure, which are then used to compute midpoint values for pressure and jet velocity and a first-order midpoint value for rocket velocity. The midpoint jet and rocket velocities are then used in (3.2f–l) to determine corrected (final) values for the compressed air volume and pressure, jet velocity, and inertial acceleration at time level $n+1$, which then lead to updates in the rocket velocity and altitude. The integration for the thrust period ends when either (i) $V_a = V_{tot}$ (all of the water gets blown out) or (ii) $p_a = p_{atm}$ (the compressed air has expanded to the minimum possible pressure).

Once the thrust period is over, the rocket is in a ballistic flight regime, and the maximum altitude and the time to reach this altitude may be computed using Bernoulli's equation if there is negligible drag force:

(3.3a)
$$z_{max} = z_{end} + w_{end}{}^2/2g \quad \text{and} \quad t_{max} = t_{end} + w_{end}/g,$$

where t_{end}, z_{end}, and w_{end} are the time, altitude, and rocket velocity at the end of the thrust period. For the case of constant drag coefficient C_d, exact integrals are

(3.3b)
$$z_{max} = z_{end} - \beta^{-1} \ln(\cos[(t_{max} - t_{end})\sqrt{\beta g}]) \quad \text{and}$$
$$t_{max} = t_{end} + \tan^{-1}(w_{end}\sqrt{\beta/g})/\sqrt{\beta g},$$

where $\beta = \rho_{atm} A_c C_d/(2m_{end})$, $\rho_{atm} = p_{atm}/(R_a T_{atm})$, and m_{end} is the total rocket mass at the end of the thrust period. For more general cases of variable drag coefficient (e.g., Reynolds number dependency) the trajectory may be determined using numerical integration as given in (3.2).

Table I   *Flight test data[3] and model predictions for rocket launches. Units are ml, psig (kPa absolute), s, degrees, and m for volume, pressure, time, angle, and height variables, respectively.*

Launch	$V_w(0)$	$p_a(0)$	$t_{max}^{\dagger}$	$\theta_{max}^{\dagger}$	$z_{max}^{\dagger}$	$z_{max}^{\ddagger}$	$t_{max}^{\ddagger}$
1	23.2	39 (370)	$(3.7)^{\S}$	23.5¶	11.2	10.41	(3.02)
2	13.2	40 (375)	(2.6)	16.0	7.8	6.05	(2.34)
3	32.2	44 (405)	1.6	28.0	13.4	13.54	1.71
4	32.2	44 (405)	1.7	30.0	14.4	13.54	1.71
5	7.2	40 (375)	*	(7 ft)	2.1	2.52	0.73
6	32.2	60 (515)	1.8	40	20.4	20.26	2.07

†field test data, ‡model prediction.

§The timings shown in columns 4 and 8 are from the moment of launch to maximum height, except for the first two launches, which are in parentheses—these times are to impact with the ground.

¶Column 5 gives the angle of maximum height, with the exception of launch 5, which gives actual maximum height (2.1 m). The baseline for the triangulation was 75 ft (23 m), and the protractor was on a tripod 4 ft (1.2 m) above ground level.

4. Results. The model solution was compared against flight test data collected by the class. The rocket tested had a dry mass and total volume of $m_s = 19.1$ g and $V_{tot} = 73.6$ ml, respectively. These measurements were made using an electronic balance (accuracy of ± 0.1 g) and graduated cylinder (accuracy of ± 0.2 ml). The rocket's nozzle exit radius was $R_{ex} = 2.5$ mm, giving $A_{ex} = 1.96 \times 10^{-5}$ m^{-2}. Atmospheric and air properties were $p_{atm} = 101$ kPa, $R_a = 287$ J $\cdot$ kgK, $\gamma = 1.40$, and $T_{atm} = 80°$ F (300 K). All launches were close to ground level, so $z_o = 0$ m, $g = 9.81$ ms^{-2}, and $\rho_w = 1000$ kg $\cdot$ m^{-3}. Sufficient time was given between launches for the compressed air and water inside the rocket to come into thermal equilibrium with the surroundings, so $T_a(0) \equiv T_{atm}$. Four distinct initial volumes of water $V_w(0)$ were used in the field tests; these volumes were marked on the rocket shell. Measurements with the graduated cylinder demonstrated a repeatability of ± 0.5 ml using these marks. The initial value of $p_a(0)$ was measured with a mechanical pressure gauge in psig, which was converted into absolute pressure in kPa for the model computations. The maximum height reached in a launch was measured using a large protractor (e.g., a unit power theodolite) and timings were made using a digital stopwatch. Table 1 shows the data collected during one class period of sufficient quality to make quantitative comparisons with the model possible.

---

[3]The accuracy of the flight test data is difficult to assess using traditional analysis methods like propagation of error because the uncertainties in crucial measurements such as the angle of maximum height were not estimated due to time constraints to keep the measurements to one class period. However, from Figure 3 it is clear that the flight data fit the model predictions for maximum heights to about 1 m, on average (in particular, note that launches 3 and 4 had the same initial state). Unless we were very lucky, this should be a reasonable estimate of the mean error of measurement. We tried to be *very meticulous* in launching and measuring the rocket. It is easy to get data that vary wildly for launches that are not done with enough care. Some suggestions are to (i) make sure the water temperature is at the ambient, (ii) check that the seal between the pressurized rocket chamber and the air pump does not leak, (iii) check that either the pressurized rocket chamber and/or the air pump themselves do not leak, (iv) practice measuring water volumes used to charge the rocket until repeatable to ± 1 ml or better, (v) attach a pressure gauge to the air pump (most easily done at the end where the rocket is seated) to allow accurate determination of the chamber pressure, and (vi) make altitude, distance, and time measurements in pairs and throw out all cases where the two sets of measurements are wildly different.
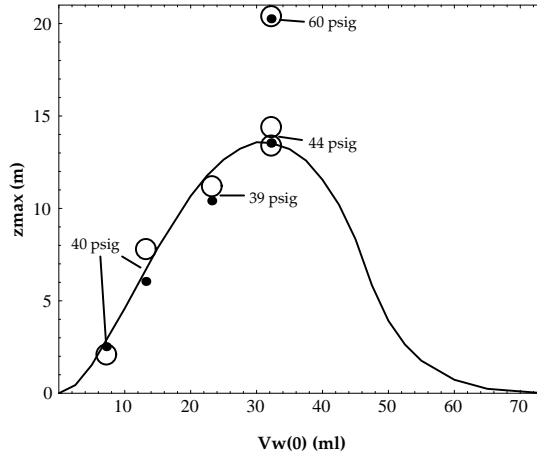
Fig. 3 *Comparison of model predictions and field tests showing maximum altitudes (m) attained by the rocket as a function of initial volume of water $V_w(0)$. Field tests (open circles) and corresponding model predictions (dots) show initial gauge pressures $p_a(0)$ (see Table 1 for equivalent absolute pressures in SI units). The solid curve is the model prediction for the single initial pressure of 44 psig (405 kPa absolute).*

In the model computations, the mass of compressed air was ignored. This was a good approximation because $m_a \sim 0.1$ g is much smaller than the masses of the water and rocket shell. The drag force term was also dropped as the ratio of drag force to thrust was $\sim 10^{-3}$. Note that this approximation decouples the interior dynamics of the rocket from its motion through the atmosphere. Resolving the thrust period into 5 to 10 timesteps typically resulted in numerical convergence (in the sense of $\Delta t \to 0$) of the solution to three to four significant figures. For launches 3–5, the thrust period lasted 0.095 s and a timestep of $\Delta t = 0.01$ s yielded a solution converged to four significant figures. The end of thrust conditions (i) $V_a = V_{tot}$ or (ii) $p_a = p_{atm}$ requires special treatment since these conditions are not met exactly on a computational timestep. For the first condition, the algorithm will predict a negative water volume. A linear interpolation based upon this negative $\widetilde{V}_w$ and the last positive value V_w^n was used to determine the end of thrust time, t_{end}, and all relevant variables were extrapolated to this time. The compressed air pressure, $p_{a,end}$, will generally be greater than p_{atm} and so there will be a sudden adjustment in p_a as the last bit of water is blown out of the chamber. In the model, no thrust is computed due to this adjustment. For the second condition, the algorithm will predict a gauge pressure less than zero. A linear interpolation based upon this negative $(\widetilde{p}_a - p_{atm})$ and the last positive value $(p_a^n - p_{atm})$ was used to determine t_{end}, and all relevant variables were extrapolated to that time. In this end state, there is a residual volume of water left in the chamber.

5. Discussion. Figure 3 shows the maximum heights the rocket reaches as predicted by the model for an initial pressure of $p_a(0) = 44$ psig (405 kPa absolute) for the range of initial water volumes $0 \leq V_w(0) \leq V_{tot}$. It shows that for a given $p_a(0)$, there exists an optimum water volume $V_{w,opt}(0)$ for which the rocket will rise higher than for any other value of $V_w(0)$. At $p_a(0) = 44$ psig this optimum volume is $V_{w,opt}(0) = 30.7$ ml, and the corresponding maximum height is $z_{max} = 13.59$ m. Figure 3 also shows the flight test data listed in Table 1 and the corresponding model predictions. Overall agreement is remarkably good.

For any given $p_a(0)$, there exists a critical water volume $V_{w,crit}(0)$ such that both ends of thrust conditions (i) and (ii) are met simultaneously. In this end state, the compressed air pressure reaches the ambient pressure precisely as the last bit of water is blown out of the chamber. For $p_a(0) = 44$ psig, this critical volume is $V_{w,crit}(0) = 46.2$ ml. The maximum height attained in this case is only 7.2 m, well below the value for $V_{w,opt}(0)$.

This problem presents numerous opportunities for refinements on the physical model. One could easily keep in terms like the compressed air mass and drag force and directly assess their effects. For students unsure of the suitability (or meaning) of an adiabatic expansion, an alternate isothermal expansion can be computed by setting $\gamma = 1$ in (2.8). For the initial conditions of launches 3–4, an isothermal expansion results in a maximum altitude of 17.3 m, well above the measured values. The isothermal expansion results in z_{max} that are too high because it requires that additional stored energy be transferred into the compressed air by heat transfer. One parameter that is difficult to measure accurately is the jet nozzle radius simply because it is so small. A probable error of 0.2 mm in the value of R_{ex} means an error of 20% in A_{ex}. Fortunately, the model is fairly insensitive to the exact value of A_{ex}. For the initial conditions of launches 3–4, values of $R_{ex} = 2.0$ and 3.0 mm produce z_{max} that are lower and higher than the value listed in Table 1 by only 0.41 and 0.25 m, respectively. A related issue is the effect of a *vena contracta* [1], which can easily be modeled by a reduction in the value of R_{ex}. Finally, improvements can be made upon the use of Bernoulli's equation. One possibility is to introduce a nozzle efficiency, $\eta < 1$, such that (2.7) is replaced by

$$(2.7')\qquad\qquad\qquad w_{ex} = \sqrt{2\eta[p_a(t) - p_{atm}]/\rho_w}.$$

If $V_w(0) < V_{w,crit}(0)$, then during the last moments of the thrust period the velocity of the air/water interface approaches w_{ex} and unsteadiness becomes important. This means that Bernoulli's equation is no longer valid (and hence (2.7), (2.7′) are suspect) as $t \to t_{end}$ from below. Nevertheless, the model solution matches the data well, suggesting that the overall impact of this unsteadiness is minimal.

For students and instructors interested in additional mathematical aspects of the model, one could solve the nonlinear integral equation (2.9) directly rather than the corresponding (2.5), (2.7), and (2.8). By considering unsteady two-dimensional flows, one could consider axisymmetric viscous flows inside and outside (a boundary layer computation) the rigid shell to more accurately determine viscous effects. At this level, the problem becomes a good test for an advanced graduate-level course in computational methods.

REFERENCES

[1] I. H. SHAMES, *Mechanics of Fluids*, McGraw-Hill, New York, 1962, pp. 109, 162.
[2] W. KAPLAN, *Advanced Calculus*, Addison-Wesley, Reading, MA, 1973, p. 337.
[3] R. WEINSTOCK, *Calculus of Variations*, Dover, New York, 1974, p. 16.
[4] H. LAMB, *Hydrodynamics*, 6th ed., Dover, New York, 1945, pp. 12, 21, 22.
[5] R. COURANT AND D. HILBERT, *Methods of Mathematical Physics*, Vol. 1, Interscience, New York, 1953, pp. 112, 185.